Robust Estimation of Fetal Heart Rate Variability Using Doppler Ultrasound

Kumari L. Fernando*, *Student Member, IEEE*, V. John Mathews, *Fellow, IEEE*, Michael W. Varner, and Edward B. Clark

***Abstract*—This paper presents a new measure of heart rate variability (HRV) that can be estimated using Doppler ultrasound techniques and is robust to variations in the angle of incidence of the ultrasound beam and the measurement noise. This measure employs the multiple signal characterization (MUSIC) algorithm which is a high-resolution method for estimating the frequencies of sinusoidal signals embedded in white noise from short-duration measurements. We show that the product of the square-root of the estimated signal-to-noise ratio (SNR) and the mean-square error of the frequency estimates is independent of the noise level in the signal. Since varying angles of incidence effectively changes the input SNR, this measure of HRV is robust to the input noise as well as the angle of incidence. This paper includes the results of analyzing synthetic and real Doppler ultrasound data that demonstrates the usefulness of the new measure in HRV analysis.**

***Index Terms*—Angle of incidence, heart rate variability, multiple signal characterization.**

I. Introduction

EIGHT out of one-thousand live-born infants have some form of heart defect, making it the single most common class of congenital abnormalities. Identification of these cases during early pregnancy reduces risks by timely treatment and/or planned delivery at tertiary care centers. Currently, the heart rate variability (HRV) analysis is used to understand the hemodynamic state in adults and children [1]–[3]. The use of fetal heart rate as a tool for monitoring fetal hemodynamics was first suggested in the 1950s using electrocardiographic (ECG) signals [4, pp. 1–6]. Unfortunately, there is no reliable or noninvasive method for measuring fetal ECG during early stages of pregnancy. Fetal ECG signals can be measured externally from electrodes placed on the maternal abdomen [4, pp. 28–54], [5]–[8]. However, these signals are in general corrupted by the maternal ECG and other signals such as abdominal action potentials. They are also significantly attenuated by tissues between the heart and the electrodes. The poor signal-to-noise ratio (SNR), and the high rate of coincidence of maternal and fetal ECG's limits the detection rate of fetal QRS complexes from these composite signals to about 60% [7], [8]. Furthermore, fetal ECG can be measured using this method only after 20 weeks of gestation [8]. Fetal ECG signals can also be measured directly from the fetal scalp [4, pp. 28–54]. However, this method is not feasible until later in gestational age and is performed after the membrane rupture.

This paper is concerned with developing a robust measure HRV from Doppler ultrasound measurements of fetal blood flow velocity waveforms. Ultrasonography is a safe, noninvasive, and cost-effective tool for monitoring fetal cardiovascular system through imaging and blood flow velocity measurements [8]–[18]. Splunder, *et al.* have shown that blood flow velocity waveforms can be measured from fetal arteries as early as the eighth week of gestation using transvaginal Doppler ultrasound techniques [14]. Short-term temporal [15] and spectral [16], [17] variability of fetal heart rate have been used for the assessment of cardiovascular development in fetuses during early human pregnancy using the umbilical arterial Doppler ultrasound blood flow measurements. Instantaneous fetal heartbeats were estimated from these blood velocity waveforms using a threshold detection scheme and spectral dynamics of beat-to-beat variability were characterized using fast Fourier transform (FFT) techniques. It is well known that the variance of the spectrum estimate based on the FFT of a random signal (periodogram) is of the order of the spectrum of the signal [19], [20, pp. 63–105]. Furthermore, the spectral resolution of FFT-based techniques is inversely proportional to the length of the data segments [20, pp. 63–105], [21, pp. 23–83]. Both these factors contribute to the unreliability of FFT-based algorithms in HRV analysis. Exposure to ultrasound beam for long durations of time may cause temperature increase and damage in fetal tissues especially in the brain encased in the fetal skull. Consequently, long-term monitoring of blood velocity waveforms is not recommended [22]. Other sources of error in HRV estimation from blood flow velocity waveforms measured using Doppler ultrasound techniques are: 1) variations in the angle between the incident ultrasound beam and the blood flow; 2) the nonuniform insonation of the vessel; 3) the high-pass filtering of the received ultrasound signal (to demodulate the Doppler signal); and 4) the SNR of the Doppler signal [12]. These factors make it difficult to define a specific reference point in each pulse in the blood velocity waveform to estimate individual heartbeats and, hence, the beat-to-beat variability.

This paper presents a solution to the problems in characterizing the HRV because of variations in the angle of insonation

Manuscript received July 30, 2002; revised January 26, 2003. This work was supported in part by the Primary Children's Medical Center Foundation, Salt Lake City, Utah under an Innovative Research Grant and in part by the Western States Affiliate of the American Heart Association under Predoctoral Fellowship 0110005Y. Parts of this work were accepted for presentation at ICASSP 2003, Hong Kong. *Asterisk indicates corresponding author.*

*K. L. Fernando is with the Department of Electrical and Computer Engineering, University of Utah, 50 S. Central Campus Dr., Room 3280 MEB, Salt Lake City, UT 84112 USA (e-mail: fernando@eng.utah.edu).

V. J. Mathews is with the Department of Electrical and Computer Engineering, University of Utah, Salt Lake City, UT 84112 USA.

M. W. Varner is with the Department of Obstetrics and Gynecology, University of Utah, Salt Lake City, UT 84132 USA.

E. B. Clark is with the Departments of Pediatrics, Bioengineering, and Obstetrics and Gynecology, University of Utah, Salt Lake City, UT 84132 USA.

Digital Object Identifier 10.1109/TBME.2003.814528

and noise levels in the Doppler signal described above. We used maximum blood flow velocity waveforms estimated from Doppler measurements in our analysis. These waveforms are not significantly affected by the nonuniform insonation and the high-pass filter settings [23]. We first demonstrate that blood velocity waveforms can be modeled as a single sinusoid embedded in white noise over short intervals of time. This model allows us to estimate the heart rate as the instantaneous frequency of the sinusoid in the short data interval. We then define the HRV as the temporal variability of the estimated heart rates over all the short intervals into which the blood velocity waveform is segmented. We use the MUSIC algorithm [21, pp. 139–160] to estimate the frequency and amplitude of the signal as well as the variance of the noise component in the signal. MUSIC is an eigenanalysis-based frequency estimation algorithm. A brief introduction to the MUSIC algorithm is given in the appendix. Unlike FFT-based methods, the spectral resolution of the estimates is not limited by the duration of the signal in this approach. Finally, we use a normalization of the temporal variations in the estimated parameters to develop a measure of HRV that is robust to the ambient noise and the angle of incidence of the ultrasound beam.

The rest of the paper is organized as follows. We describe the robust measure of HRV in Section II. Experimental results verifying the robustness properties of the measure is provided in Section III. The concluding remarks are given in Section IV.

II. HRV Analysis

A. Signal Modeling

Fig. 1 depicts a portion of an umbilical arterial blood velocity waveform acquired from an 18-week-old fetus. The temporal characteristics of the waveform suggest that this signal can be modeled as a pure sinusoid embedded in white noise over a short duration of time. Such inference can be further justified when we consider the autocovariance function of the signal. Fig. 2 shows the unbiased sample autocovariance function of the signal in Fig. 1. Since the estimated autocovariance function appears to match the sinusoidal model, we model the autocovariance function of the fetal blood velocity waveforms as a pure sinusoid embedded in noise over short intervals. We note that the harmonic frequencies of the heart rate are of relatively low strength compared with the fundamental and are further attenuated in the covariance function due to the squaring effect. In our approach, we study the temporal variations in the characteristics of the velocity waveforms using the frequency and amplitude values estimated from its autocovariance function using the MUSIC algorithm. The amplitude and the frequency values evaluated by the algorithm correspond to the instantaneous peak blood velocity and heart rate values, respectively.

B. A Robust Heart Rate Variability Measure

The instantaneous blood flow velocity estimated using Doppler ultrasound is given by

$$\nu(t) = \frac{cf(t)}{2f_o \cos\theta(t)} \tag{1}$$

where c is the velocity of ultrasound in the medium, f_o is the ultrasound frequency, $f(t)$ is the Doppler shift, and $\theta(t)$ is the angle of incidence at time t. We sample blood velocity waveforms at a sampling frequency such that half of the sampling frequency is much greater than the expected highest heart rate and then divide each waveform into short segments of time corresponding to two to three heartbeats. We assume that the instantaneous peak velocity, frequency and the angle of incidence do not change significantly over these short segments. Let, M be the number of samples per segment and N be the number of such segments in the blood velocity waveform. Consequently, we can model the nth velocity sample of the ith segment using

$$\nu(i,n) = \alpha_i \cos(2\pi f_i n + \phi_i)\cos\theta_i + \xi(n); \begin{cases} 0 \le n \le M-1 \\ 1 \le i \le N \end{cases} \tag{2}$$

where f_i, α_i, and ϕ_i are the instantaneous frequency, the amplitude and the phase values of the velocity waveform, θ_i is the instantaneous value of the angle of incidence, and $\xi(n)$ is an independent identically distributed (IID) noise process with zero mean value and variance σ_ξ^2. Similarly, we assume that the statistics of the noise process $\xi(n)$ changes slowly compared with the variations in the frequency and the velocity of the waveform.

Let, $\hat{\alpha}_i$, $\hat{f}_i$, and $\hat{\sigma}^2_{\xi,i}$ denote the estimated amplitude, frequency and the noise variance, respectively, for the ith block.

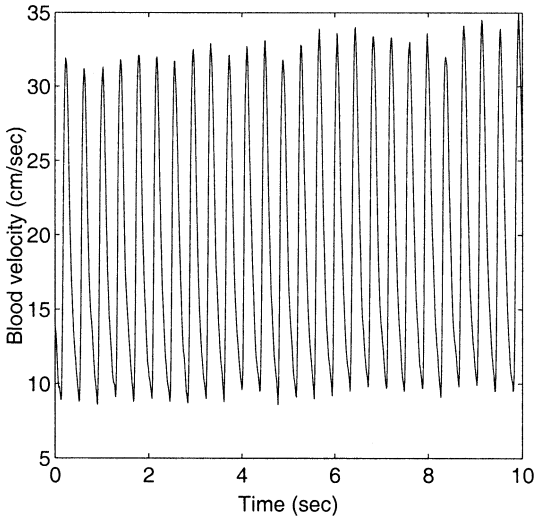

Fig. 1. Umbilical arterial blood velocity of a fetus at 18 weeks of gestation.

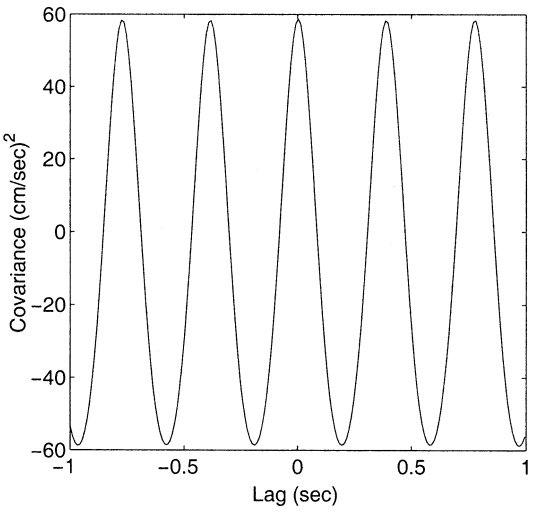

Fig. 2. Sample function of the signal in Fig. 1.

We note that $\hat{\alpha}_i$ is an estimate of $\alpha_i \cos\theta_i$ in (2). Then, an estimate of the SNR for the signal in the ith segment is given by

$$\mathrm{SNR}_i = \frac{\hat{\alpha}_i^2}{2\hat{\sigma}_{\xi,i}^2}. \tag{3}$$

From the above discussion, it is clear that the SNR is directly proportional to $\cos^2\theta_i$ when all the other parameters are fixed. For a complex-valued sinusoid embedded in white noise, Kay [20, pp. 407–445] has empirically shown that the mean-square error (MSE) in estimating the frequency using MUSIC is inversely proportional to the SNR of the input signal. This result can be extended to the case of real sinusoids to show that the MSE is inversely proportional to the square root of the SNR.

Therefore, we can eliminate the dependence of the MSE on the angle of incidence by defining a normalized HRV measure as

$$\mathrm{NHRV} = \left[\frac{1}{N}\sum_{i=1}^{N}\left\|\hat{f}_i - \mu_f\right\|^2 \sqrt{\mathrm{SNR}_i}\right]^{1/2} \tag{4}$$

where μ_f is the mean heart rate computed over the whole waveform. In contrast, an estimate of the HRV given by

$$\mathrm{HRV} = \left[\frac{1}{N}\sum_{i=1}^{N}\left\|\hat{f}_i - \mu_f\right\|^2\right]^{1/2} \tag{5}$$

depends significantly on the measurement noise as well as the angle of incidence. Therefore, this un normalized measure cannot provide reliable information about the cardiovascular system.

III. Experimental Results

In this section, we verify the properties of the normalized HRV measure in two ways. The first set of experiments involves simulated and real Doppler signals collected for different angles of incidence. We demonstrate that the normalized HRV shows little dependence on the measurement noise level and the angle of incidence. The second set of experiments involves the analysis of fetal umbilical arterial blood velocity waveforms. We show through the analysis of 108 waveforms obtained from fetuses aged 10–20 weeks of gestation that the evolution of the normalized HRV with gestational age agrees with the known physiological behavior of HRV in fetuses.

A. Verification of Robustness to Angle of Incidence and Measurement Noise

A synthetic signal modeled as in (2) was generated with $f_i = 150$ beats-per-minute (b/min), $\alpha_i = 10$ cm/s and a sampling frequency of 100 samples/s. The angles of incidence was varied from $-80°$ to $+80°$ in steps of $2°$. One-thousand independent experiments were performed at each angle θ_i and the experiments were repeated for noise variance values $\sigma_\xi^2 = 0.001, 0.01$, and 0.1. Each experiment employed 110 samples. The MUSIC algorithm was employed to estimate the instantaneous frequencies of the signal.

Fig. 3 depicts the variation of the estimated mean frequency values for the above three variance values with the angle of incidence. This demonstrates that we can estimate the heart rate accurately for large ranges of noise variances and angles of incidence.

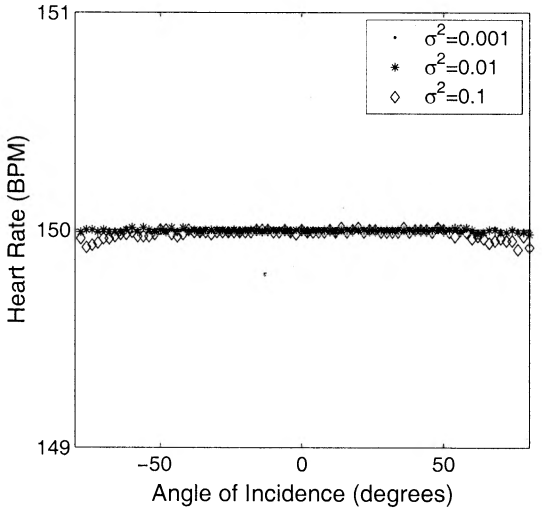

Fig. 3. Distributions of the estimated mean heart rate.

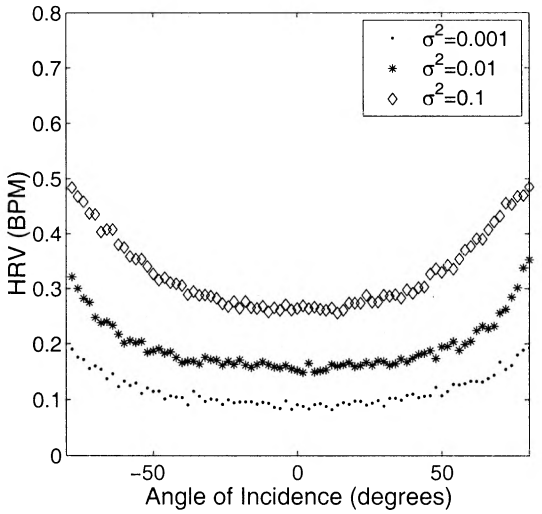

Fig. 4. Distribution of the HRV with the angle of incidence.

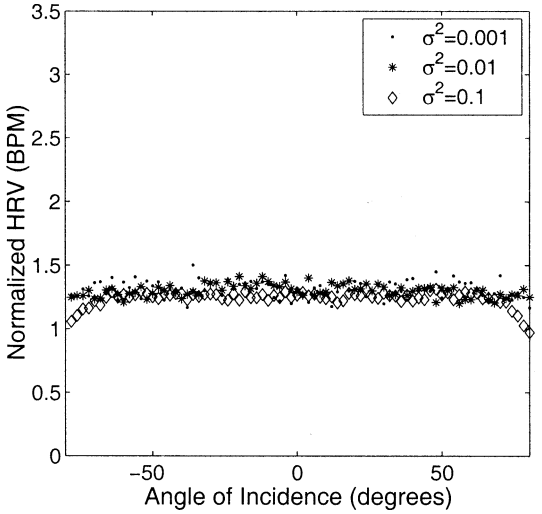

Fig. 5. Distribution of the normalized HRV with the angle of incidence.

At each angle θ, the HRV was estimated as the root mean square (RMS) deviation of the frequency estimates from their mean value and the normalized HRV was computed using (4) over the 1000 estimates. Figs. 4 and 5 display the HRV and

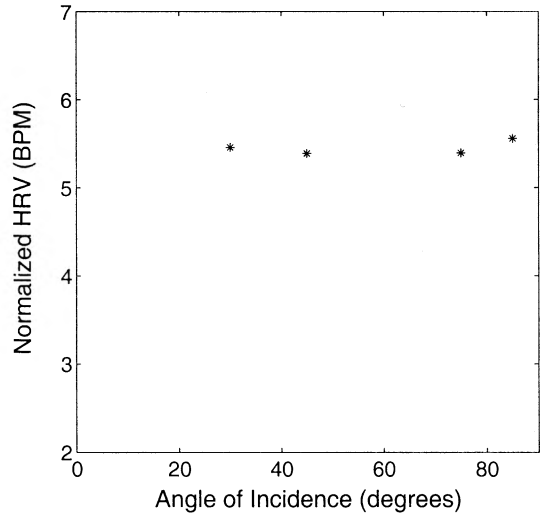

Fig. 6. Distribution of the normalized HRV estimated for the carotid arterial blood velocity with the angle of incidence.

the normalized HRV, respectively, as functions of the angle of incidence for the three different noise levels. We can see from these results that the normalized HRV measure is relatively independent of the angle of incidence as well as the noise variances.

We also evaluated the normalized HRV using blood velocity waveforms measured at different incident angles from a carotid artery of an adult. Fig. 6 shows the normalized HRV values at four different incidence angles. From this figure, it can be concluded that the normalized HRV measure is relatively constant with the angle of incidence.

B. Evolution of Fetal HRV With the Gestational Age

In normal fetuses, changes in heartbeat patterns with the gestational age can be explained using physiological considerations. Myofibrils in the cardiac muscle are responsible for the contractility of the myocardium. The increase in the number of myofibrils increases efficiency of the myocardial contractility. By 8–10 weeks of the gestational age myofibrils appears in large numbers improving the contractility of the myocardium and, hence, decreasing the heart rate [15]. The autonomic nervous system develops first with the parasympathetic nervous system which matures around 15 weeks of gestation. The parasympathetic nervous system activity tends to decrease the heart rate. Due to both these factors, heart rate decreases from 10 to 15 weeks of gestation and remains approximately constant from 15 to 20 weeks [24]. Similarly, the HRV remains approximately constant from 10 to 15 weeks and increases from 15 to 20 weeks of gestation. The increased HRV with fetal age is due to the maturation of the parasympathetic limb of the autonomic nervous system around the 15th week of fetal life [24]. Development of other oscillatory mechanisms of the body such as respiration, baroreceptor, and vasomotor may also influence the increase in the HRV [15]. In what follows, we show using ultrasound blood flow velocity waveforms collected from 108 fetuses between 10 and 20 weeks of gestational age that the evolution of the normalized HRV measure is similar to the behavior predicted based on the physiological considerations. This demonstration further strengthens the claim that the normalized HRV measure of this paper is a viable candidate of assessing fetal cardiovascular health.

1) Data Acquisition: The fetal ultrasound measurements were collected at the Department of Obstetric and Gynecology, Academic Hospital Rotterdam-Dijkzigt, Rotterdam, The Netherlands. This study was approved by the Hospital Ethics Committee at the Erasmus University. Of the women who consented to participate in the study, there were 108 women with normal singleton pregnancy between 10 and 20 weeks of gestation. Ten fetuses were studied in each age group (each week of gestation within 10 to 20 weeks) except for week 19 where only 8 data sets were available. All pregnancies were uncomplicated and infants were normal with a birth weight between the 10th and the 90th percentile corrected for maternal parity and sex. The angle of incidence was kept below 20° and the flow velocity waveforms were obtained from the free floating loop of the umbilical artery. Transvaginal (5 MHz) and tranabdominal (3.75 MHz) Doppler recordings were used at 10–13 and 14–20 weeks of gestation, respectively. All Doppler studies were performed for 18 to 45 s with the women in the semi-recumbent position and during fetal apnea. Consequently, all waveforms consisted of more than 40 beats and were adequate for the HRV analysis.

Umbilical arterial Doppler signals were stored in superVHS (sVHS) tapes in PAL format using a Panasonic superVHS video cassette recorder (model AG7350) with near CD quality audio. The recorded audio signals were digitized offline at 12 kHz using a 12-bit analog-to-digital converter (National Instruments) and acquired using a personal computer. The digitized signals were first divided into segments containing 512 samples with 75% overlap so that the signal parameters were estimated at every 128 samples. Therefore, the sampling frequency of the reconstructed waveforms was 93.75 samples/s. The maximum velocity envelope was estimated using the FFT-based threshold crossing algorithm described in [23].

In a separate study, Doppler ultrasound measurements were made using the same algorithm on 11 normal fetuses of 10- to 20-week gestation during three successive 5-min intervals to evaluate the dependence of instantaneous state of the fetus on the reproducibility of the flow velocity parameters. There was no statistically significant difference in the umbilical arterial flow velocity parameters estimated from the three separate sets of measurements.

The spectral analyses of the fetal heart rate time series have shown that between 10 and 20 weeks gestational age, a significant portion of signal spectrum exists below 1 Hz [17]. This indicates that the instantaneous peak velocity and heart rate do not change significantly over short intervals of time less than 1 s during 10–20 weeks of gestation. In this work, we estimate the instantaneous heart rate values using intervals approximately of1 s (90 samples) corresponding to two to three heartbeats. We also assume that the angle of insonation remains constant over this interval of time. The input to the MUSIC algorithm consisted of the autocovariance function of each block for the lags in the range $[-35, 35]$. The algorithm then estimated the autocovariance of this data for lags in the range [0, 10], and from that estimated the frequency and the amplitude of a single

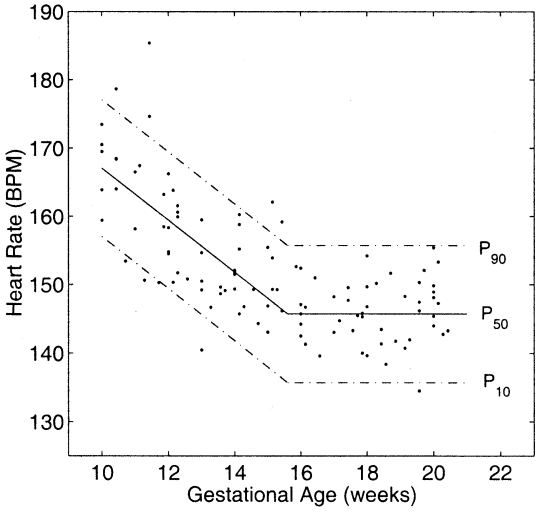

Fig. 7. The distribution of the heart rate as a function of the age.

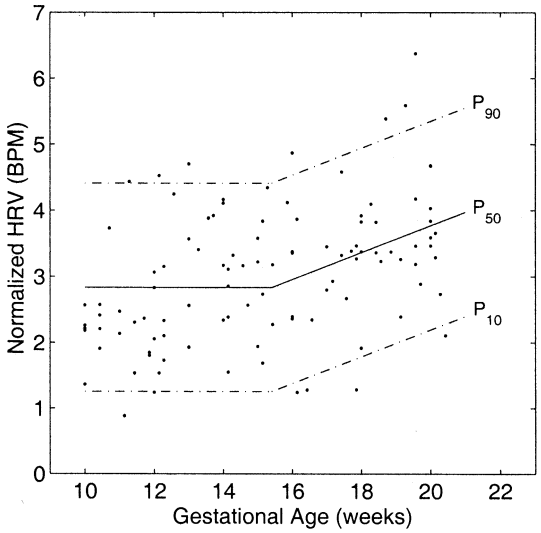

Fig. 8. Normalized heart rare variability as a function of the age.

real sinusoid in the model along with the variance of the noise component.

2) Mean Heart Rate: Fig. 7 depicts the mean value of the estimated instantaneous heart rates for each waveform as a function of the gestational age. As expected, the mean heart rate decreased linearly with gestational age up to the 15th week and then remained approximately constant. The piecewise-linear model of the mean heart rate estimated using the least-squares curve fitting for ages 10 to 15 weeks and 15 to 20 weeks of gestation is the solid line in the figure (P_{50}). The relationship of the estimated model for the mean heart rate $\bar{f}$ with the gestational age ω over the period of 10–20 weeks of gestation was given by

$$\bar{f}(\omega) = \begin{cases} -3.8076\omega + 205.1209, & 10.0 \le \omega \le 15.4 \\ 146.4839, & 15.4 \le \omega \le 20.0. \end{cases} \quad (6)$$

The RMS deviation of the mean heart rates from this model was 6.10 beats/min. Fig. 7 also shows the 90% confidence intervals (P_{10} and P_{90}) for the distribution of the mean heart rates assuming that variations are Gaussianly distributed.

3) Normalized Heart Rate Variability: The variability of the heart rate estimates were characterized using the normalized RMS deviation of the estimated mean heart rate over each waveform , calculated using (4). Fig. 8 depicts the behavior of the normalized HRV with the gestational age. The solid line (P_{50}) shows the piecewise-linear least-squares fit of the HRV with the gestational age and is given by

$$\Delta_f(\omega) = \begin{cases} 2.8307, & 10.0 \le \omega \le 15.4 \\ 0.2040\omega - 0.3109, & 15.4 \le \omega \le 20.0. \end{cases} \quad (7)$$

In the first segment (from week 10 to 15), the HRV was constant. In the second segment (from week 15 to 20), the HRV gradually increased. The estimated RMS deviation of the data from this model is 0.96 beats/min. The 90% confidence intervals (P_{10} and P_{90}) of the estimation are marked by the dotted lines.

Both the estimated heart rate and the HRV evolve with the gestational age as expected according to the physiological considerations. This, in conjunction with its robustness properties, makes the normalized HRV measure more useful for assessing fetal cardiovascular function than its un normalized counterparts.

IV. Conclusion

Reliable estimation of the frequency components of nonstationary data is difficult with Fourier transform-based algorithms when data lengths are short. Furthermore, HRV measures based on the Doppler ultrasound measurements have been handicapped in the past because of their dependence on the measurement noise and the angle of incidence of the ultrasound beam. The normalized HRV measure based on frequency estimation using the MUSIC algorithm is robust to variations in the angle of incidence of the ultrasound beam as well as the measurement noise. This is a significant advantage of our approach over the current state-of-the-art in HRV measurement. Furthermore, real-time implementation of our algorithm is not difficult. As a result of these observations, we believe that the normalized HRV is an excellent candidate for assessing fetal cardiovascular health. Preliminary results of using the normalized HRV as a marker for abnormal cardiovascular development suggest that fetuses with severe congenital heart defects have HRV measures different from fetuses with structurally normal hearts. Confirmation of these findings would open the possibility of intervention and therapy at a sufficiently earlier gestational age than current mid-trimester techniques. In addition, many women at increased risk for a fetus with congenital heart disease could be reassured at an earlier gestational age than is currently possible.

Appendix

The MUSIC algorithm [20, pp. 407–445], [21, pp. 139–160] is briefly explained here. Let $y(n)$ be a real-valued signal modeled as a sum of P sinusoids in noise as

$$y(n) = \sum_{k=1}^{P} \alpha_k \cos(2\pi f_k n + \psi_k) + \xi(n) \quad (A.8)$$

where $\xi(n)$ is an IID process with zero mean value. The parameters α_k and f_k represent the amplitude and the frequency

of the kth sinusoid of the signal, respectively. We assume that $f_k \neq f_m$ for $k \neq m$. The phase ψ_k is assumed to be uniformly distributed over $[0, 2\pi)$ radians and uncorrelated with ψ_m for $k \neq m$. In the analysis model of (2), $P = 1$, but the following discussion assumes an arbitrary value of P.

The signal $y(n)$ has zero mean value. The covariance function of the random process $y(n)$ is given by

$$\gamma_{yy}(m) = \sum_{i=1}^{P} \frac{\alpha_i^2}{2} \cos 2\pi f_i m + \sigma_\xi^2 \delta(m). \tag{A.9}$$

Let $x(n)$ denote the sinusoidal components in $y(n)$, i.e.,

$$x(n) = \sum_{k=1}^{P} \alpha_k \cos\left(2\pi f_k n + \psi_k\right). \tag{A.10}$$

The covariance function γ_{xx} of $x(n)$ is given by

$$\gamma_{xx}(m) = \sum_{i=1}^{P} \frac{\alpha_i^2}{2} \cos 2\pi f_i m. \tag{A.11}$$

Since each sinusoid can be represented as a summation of two complex sinusoids using the relationship

$$\cos 2\pi f m = \frac{e^{j2\pi f m} + e^{-j2\pi f m}}{2} \tag{A.12}$$

$\gamma_{xx}(m)$ can be represented as a summation of $2P$ frequency components as

$$\gamma_{xx}(m) = \sum_{i=1}^{2P} \left(\frac{\alpha_i}{2}\right)^2 e^{j2\pi f_i m} \tag{A.13}$$

where $f_{i+P} = -f_i$ and $\alpha_{i+P} = \alpha_i$ for $1 \leq i \leq P$. Substituting (A.13) in (A.9) results in

$$\gamma_{yy}(m) = \sum_{i=1}^{2P} \left(\frac{\alpha_i}{2}\right)^2 e^{j2\pi f_i m} + \sigma_\xi^2 \delta(m). \tag{A.14}$$

Let the frequency vector

$$\mathbf{a}(f) = [1 \quad e^{-j2\pi f} \quad e^{-j4\pi f} \quad \cdots \quad e^{-j2(m-1)\pi f}]^T \tag{A.15}$$

where $m > 2P$. Let us further define the matrix of all the frequency vectors

$$\mathbf{A} = [\mathbf{a}(f_1) \quad \mathbf{a}(f_2) \quad \cdots \quad \mathbf{a}(f_{2P})]. \tag{A.16}$$

The rank of the matrix $\mathbf{A}$ is equal to the number of distinct sinusoids $2P$ in the signal.

Let us consider the m-component signal vectors given by

$$\begin{aligned}\tilde{\mathbf{y}}(n) &= [y(n) \quad y(n-1) \quad \cdots \quad y(n-m+1)]^T \\ &= \mathbf{A}\tilde{\mathbf{x}}(n) + \tilde{\xi}(n),\end{aligned} \tag{A.17}$$

where

$$\tilde{\mathbf{x}}(n) = [x_1(n) \quad x_2(n) \quad \cdots \quad x_{2P}(n)]^T \tag{A.18}$$

and

$$\tilde{\xi}(n) = [\xi(n) \quad \xi(n-1) \quad \cdots \quad \xi(n-m+1)]^T. \tag{A.19}$$

The covariance matrix of the signal vector $\tilde{\mathbf{y}}(n)$ is

$$\begin{aligned}\mathbf{R} &= \mathcal{E}\{\tilde{\mathbf{y}}(n)\tilde{\mathbf{y}}^*(n)\} \\ &= \mathbf{A}\mathbf{P}\mathbf{A}^H + \sigma_\xi^2 \mathbf{I}_{m,m}\end{aligned} \tag{A.20}$$

where

$$\mathbf{P} = \begin{bmatrix} \left(\frac{\alpha_1}{2}\right)^2 & 0 & \cdots & 0 \\ 0 & \left(\frac{\alpha_2}{2}\right)^2 & \cdots & 0 \\ \vdots & \cdots & \ddots & \vdots \\ 0 & \cdots & \cdots & \left(\frac{\alpha_{2P}}{2}\right)^2 \end{bmatrix} \tag{A.21}$$

$\{\cdot\}^H$ is the Hermitian transform of $\{\cdot\}$, and $\mathbf{I}_{m,m}$ is an m-dimensional identity matrix. Let $\{\lambda_1, \lambda_2, \ldots, \lambda_m\}$ denote the eigenvalues of $\mathbf{R}$ in the descending order, and $\{\mathbf{s}_1, \mathbf{s}_2, \ldots, \mathbf{s}_{2P}\}$ be the eigenvectors associated with first $2P$ eigenvalues and $\{\mathbf{g}_{2P+1}, \mathbf{g}_{2P+2}, \ldots, \mathbf{g}_m\}$ be the eigenvectors associated with $\{\lambda_{2P+1}, \lambda_{2P+2}, \ldots, \lambda_m\}$. Here

$$\lambda_k > \sigma_\xi^2 \text{ for } k = 1, 2, \ldots, 2P \tag{A.22}$$

and

$$\lambda_k = \sigma_\xi^2 \text{ for } k = 2P+1, 2P+2, \ldots, m. \tag{A.23}$$

Let

$$\mathbf{S} = [\mathbf{s}_1 \quad \mathbf{s}_2 \quad \ldots \quad \mathbf{s}_{2P}] \tag{A.24}$$

and

$$\mathbf{G} = [\mathbf{g}_{2P+1} \quad \cdots \quad \mathbf{g}_m]. \tag{A.25}$$

Then

$$\mathbf{R}\mathbf{G} = \mathbf{G}\begin{bmatrix} \lambda_{2P+1} & 0 & \cdots & 0 \\ 0 & \lambda_{2P+2} & \cdots & 0 \\ \vdots & \cdots & \ddots & \vdots \\ 0 & \cdots & \cdots & \lambda_m \end{bmatrix} = \sigma_\xi^2 \mathbf{G}.$$

However, from (A.20), we get

$$\mathbf{R}\mathbf{G} = \mathbf{A}\mathbf{P}\mathbf{A}^H\mathbf{G} + \sigma_\xi^2\mathbf{G}. \tag{A.26}$$

This implies that

$$\mathbf{A}\mathbf{P}\mathbf{A}^H\mathbf{G} = \mathbf{0}. \tag{A.27}$$

However, $\mathbf{AP}$ has full column rank implying that

$$\mathbf{A}^H\mathbf{G} = \mathbf{0}. \tag{A.28}$$

The solutions to the above equation, $\{f_k\}_{k=1}^{2P}$ are found by solving the following equation [20, pp. 407–445], [21, pp. 139–160]:

$$\mathbf{a}^H(f)\mathbf{G}\mathbf{G}^H\mathbf{a}(f) = 0 \tag{A.29}$$

or equivalently determining the angular positions of the $2P$ roots of the following equation:

$$\mathbf{a}\left(z^{-1}\right)\mathbf{G}\mathbf{G}^H\mathbf{a}(z) = 0 \tag{A.30}$$

located nearest to the unit circle, where

$$\mathbf{a}(z) = [1 \quad z^{-1} \quad z^{-2} \quad \ldots \quad z^{-(m-1)}]^T. \tag{A.31}$$

Because we consider real sinusoids, these roots will appear as complex conjugate pairs. In other words, for every frequency estimate f_i. there will be a corresponding frequency $-f_i$ estimated.

The amplitudes of the real sinusoidal components and the noise variance may then be estimated using the autocovariance

function of $y(n)$. We can expand (A.9) as a matrix equation given by

$$\begin{bmatrix} 1 & \dots & 1 & 1 \\ \cos 2\pi f_1 & \dots & \cos 2\pi f_P & 0 \\ \cos 4\pi f_1 & \dots & \cos 4\pi f_P & 0 \\ \vdots & \ddots & \vdots & 0 \\ \cos 2P\pi f_1 & \dots & \cos 2P\pi f_p & 0 \end{bmatrix} \begin{bmatrix} \frac{\alpha_1^2}{2} \\ \frac{\alpha_2^2}{2} \\ \vdots \\ \frac{\alpha_P^2}{2} \\ \sigma_\xi^2 \end{bmatrix} = \begin{bmatrix} r_{yy}(0) \\ r_{yy}(1) \\ r_{yy}(2) \\ \vdots \\ r_{yy}(P) \end{bmatrix}. \quad \text{(A.32)}$$

The amplitude in each P sinusoids under analysis and the noise variance σ_ξ^2 can be directly estimated by solving the $P+1$ linear equations in (A.32).

Then, the SNR of the signal is

$$\text{SNR} = \frac{\sum_{k=1}^{P} \frac{\alpha_k^2}{2}}{\sigma_\xi^2}. \quad \text{(A.33)}$$

ACKNOWLEDGMENT

The authors would like to thank N. T. C. Ursem, P. C. Struijk, and J. W. Wladimiroff for providing the ultrasound data.

REFERENCES

[1] Task Forceof the European Society, "Heart rate variability, standards of measurement, standards," *Circulation*, vol. 93, no. 5, pp. 1043–1065, 1996.

[2] M. B. Lotric, A. Stefanovska, D. Stajer, and V. U. Rovan, "Spectral components of heart rate variability determined by wavelet analysis," *Physiological Meas.*, vol. 21, pp. 441–457, 2001.

[3] H. L. Chan, H. S. Huang, and J. L. Lin, "Time-frequency analysis of heart rate variability during transient segments," *Ann. Biomed. Eng.*, vol. 29, pp. 983–996, 2001.

[4] R. K. Freeman and T. J. Garite, *Fetal Heart Rate Monitoring* . Baltimore, MD: Williams & Wilkins, 1981.

[5] P. P. Kanjilal and G. Saha, "Fetal ECG extraction from single channel maternal ECG using SVD and SVR spectrum," *IEEE Proc. EMBC CMBEC*, pp. 187–188, 1995.

[6] D. M. Mooney, L. J. Groome, S. B. Holland, and Y. D. Smith, "Heart rate dynamics of low risk human fetuses," *Pediatric Res.*, vol. 44, no. 1, pp. 111–118, 1998.

[7] J. H. Nagel, "Progresses in fetal monitoring by improved data acquisition," *IEEE Eng. Med. Biol. Mag.*, pp. 9–13, Sept. 1984.

[8] M. Peters, J. Crowe, J. F. Pieri, H. Quartero, B. H. Gill, D. James, J. Stinstra, and S. Shakespeare, "Monitoring the fetal heart noninvasively: A review of methods," *J. Perinatal Med.*, vol. 29, pp. 408–416, 2001.

[9] D. E. Fitzgerald and J. E. Drumm, "Noninvasive measurement of human fetal circulation using ultrasound: A new method," *Br. Med. J.*, vol. 3, pp. 1450–1451, 1977.

[10] J. E. E. Fleming, S. P. W. Raymond, G. C. S. Smith, and C. R. Whitfield, "The measurement of fetal systolic time intervals: Lessons from ultrasound," *Eur. J. Obstet., Gynecol., Reproduction Biol.*, vol. 23, pp. 289–294, 1986.

[11] F. M. Clements and N. P. deBruijn, "Noninvasive cardiac monitoring," *Crit. Care Clinics*, vol. 4, pp. 435–454, 1988.

[12] S. H. Eik-Nes, K. Marsal, A. O. Brubakk, K. Kristofferson, and M. Ulstein, "Ultrasonic measurement of human fetal blood flow," *J. Biomed. Eng.*, vol. 4, pp. 28–36, 1987.

[13] H. Feigenbaum, "Evolution of echocardiography," *Circulation*, vol. 93, no. 7, pp. 1321–1327, 1996.

[14] P. Splunder, T. Stijnen, and J. W. Wladimiroff, "Fetal atrioventricular flow-velocity waveform and their relation to arterial and venous flow-velocity waveforms at 8 to 20 weeks of gestation," *Circulation*, vol. 94, no. 6, pp. 1372–1378, 1996.

[15] N. T. C. Ursem, P. C. Struijk, W. C. J. Hop, E. B. Clark, B. B. Keller, and J. W. Wladimiroff, "Heart rate and flow velocity variability as determined from umbilical Doppler velocimetry at 10–20 weeks of gestation," *Clin. Sci.*, vol. 95, pp. 539–545, 1998.

[16] P. C. Struijk, N. T. C. Ursem, V. J. Mathews, E. B. Clark, B. B. Keller, and J. W. Wladimiroff, "Power spectral analysis of heart rate and blood flow velocity variability measured in the umbilical artery and uterine artery in the early pregnancy," *J. Ultrasound Obstet. Gynecol.*, pp. 316–322, 2001.

[17] N. T. C. Ursem, M. H. Kempski, M. A. de Ridder, P. C. Struijk, E. B. Clark, and J. W. Wladimiroff, "An estimation of fetal autonomic state by spectral analysis of human umbilical artery blood flow velocity," *Cardiovasc. Res.*, vol. 37, pp. 601–605, 1998.

[18] C. Brezinka, "Fetal hemodynamics," *J. Perinatal Med.*, vol. 29, pp. 371–380, 2001.

[19] A. H. Nuttal, "Analysis of a generalized frame work for spectral estimation—Part 2: Reshaping and variance results," *Inst. Elect. Eng. Proc.*, vol. 130, pp. 242–245, 1983.

[20] S. M. Kay, *Modern Spectral Estimation.* Englewood Cliffs, NJ: Prentice-Hall, 1988.

[21] P. Stoica and R. Moses, *Introduction to Spectral Analysis.* Upper Saddle River, NJ: Prentice-Hall, 1997.

[22] "International Society Safety statement, 2000 (reconfirmed 2002)," *J. Ultrasound Obstet. Gynecol.*, vol. 19, p. 105, 2002.

[23] N. T. C. Ursem, H. J. F. Brinkman, P. C. Struijk, W. C. J. Hop, M. H. Kempski, B. K. Keller, and J. W. Wladimiroff, "Umbilical artery waveform analysis based on maximum, mean, and mode velocity in early human pregnancy," *Ultrasound Med. Biol.*, vol. 24, no. 1, pp. 1–7, 1998.

[24] J. W. Wladimiroff and J. C. Seelan, "Fetal heart action in early pregnancy—Development of fetal vagal function," *Eur. J. Obstet. Gynecol.*, vol. 2, pp. 55–63, 1972.

Kumari L. Fernando (S '01) received the B.Sc. degree from the University of Moratuwa, Moratuwa, Sri Lanka, in electronic and telecommunication engineering in 1993 and the M.Eng. degree in telecommunication engineering from the Asian Institute of Technology, Bangkok, Thailand, in 1996. She is currently working towards the Ph.D degree in electrical engineering at the University of Utah, Salt Lake City.

Her research interests are biomedical signal processing, spectral estimation, and adaptive filters.

Ms. Fernando is the recipient of the Dorothy Penrose Stout award together with a Predoctoral Fellowship from the Western States Affiliate of the American Heart Association for the academic year 2001/2002.

V. John Mathews (S'82–M'84–SM'90–F'02) received the Ph.D. and M.S. degrees in electrical and computer engineering from the University of Iowa, Iowa City, in 1984 and 1981, respectively, and the B.E. (Hons.) degree in electronics and communication engineering from the University of Madras, Madras, India, in 1980.

At the University of Iowa, he was a Teaching/Research Fellow from 1980 to 1984 and a Visiting Assistant Professor in the Department of Electrical and Computer Engineering during the 1984–1985 academic year. He joined at the University of Utah, Salt Lake City, in 1985, where he is aProfessor of the Department of Electrical and Computer Engineering. He served as the Chairman of the Department during 2000-2003. His research interests are in adaptive filtering, nonlinear filtering, image compression, and application of signal processing techniques in communication systems and biomedical engineering. He is the author, co-authored with Professor G. L. Sicuranza, University of Trieste, Italy, of the book *Polynomial Signal Processing* (New York: Wiley, 2003).

Prof. Mathews has served as a member of the Signal Processing Theory and Methods Technical Committee, the Education Committee and the Conference Board of the IEEE Signal Processing Society. He is currently the Vice President-Finance of the IEEE Signal Processing Society. He is a past Associate Editor of the IEEE TRANSACTIONS ON SIGNAL PROCESSING, and the IEEE SIGNAL PROCESSING LETTERS. He was the General Chairman of *IEEE International Conference on Acoustics, Speech and Signal Processing* (ICASSP) 2001.

Michael W. Varner received the B.A. degree in obstetrics and gynecology from St. Olaf Collage, Northfield, MN, and the M.D. degree in maternal-fetal medicine from University of Minnesota, Minneapolis, in 1971 and 1975, respectively.

He was an Assistant Professor at the Department of Obstetrics and Gynecology, University of Iowa, Iowa City, from 1981 to 1987. From 1985 to 1987, he was also the Director of the Obstetric Service at the University of Iowa. He joined the Department of Obstetrics and Gynecology, the University of Utah, Salt Lake City, in 1987. Currently, he is a Professor of Departments of Obstetrics and Gynecology, and Pediatrics and the Director of the Division of Maternal-Fetal Medicine at the University of Utah.

Edward B. Clark was born in New York City in 1944. He received the M.D. degree from Albany Medical College, Albany, NY, and specialized in Pediatric Cardiology at the Johns Hopkins Medical Institutions in Baltimore, MD.

He is Chairman of the Department of Pediatrics at the University of Utah, Salt Lake City, and Medical Director of Primary Children's Medical Center. He currently is the Wilma T. Gibson Presidential Endowed Chair for the Department of Pediatrics and holds adjunct professorships in the Departments of Obstetrics and Gynecology and Bioengineering. He currently is a consultant to the National Institutes of Health and the National Children's Study. In Utah, he has developed an integrated coordinated program for clinical care, research, and advocacy for children with chronic illness and the prevention of disease. Dr. Clark, C. Clark, and Dr. C. Neill, are authors of *The Heart of a Child* (Baltimore, MD: Johns Hopkins Univ. Press, 1992), a best selling family reference book for parents of children with congenital heart defects.